LEGIBILITY NOTICE

A major purpose of the Technical Information Center is to provide the broadest dissemination possible of information contained in DOE's Research and Development Reports to business, industry, the academic community, and federal, state and local governments.

Although a small portion of this report is not reproducible, it is being made available to expedite the availability of information on the research discussed herein.

CONF-870962--1

Los Alamos National Laboratory is operated by the University of California for the United States Department of Energy under contract W-7405-ENG-36

LA-UR--87-3619

DE88 001802

TITLE: Computer Simulation of Pencil Glide in B.C.C. Metals

AUTHOR(S): Anthony D. Rollett, MST-6
U. Fred Kocks, CMS

SUBMITTED TO: 8th Int. Conf. on Textures of Materials,
Santa Fe, NM September 21-25, 1987

Los Alamos

Los Alamos National Laboratory
Los Alamos, New Mexico 87545

COMPUTER SIMULATION OF PENCIL GLIDE IN B.C.C. METALS

A.D.Rollett and U.F.Kocks

Los Alamos National Laboratory, NM, U.S.A.

ABSTRACT

An existing computer code for simulation of texture development in polycrystals has been modified to model "pencil glide" as observed in some b.c.c. metals. Pencil glide can be thought of as a limiting case where the slip direction is restricted to <111> directions but the slip plane is arbitrary. The existing code simulates "restricted glide", i.e. <111>{110} slip systems, by using the Bishop-Hill method (1) to find the active vertex of the single crystal yield surface for each grain. It then corrects this trial solution by using a non-linear viscous law based on the total <111>-resolved stress component. Only a small increase in computation time required is required compared to restricted glide. The results of the pencil glide modification of the code are that the texture development in tension is essentially the same as for restricted glide but that significant differences appear in plane strain compression (rolling). The Taylor Factor in tension for a random polycrystal is found to be 2.74 as previously obtained by Rosenberg and Piehler (2) and Parnière and Roesch (3).

Introduction

Many years ago it was proposed that the deformation of single crystals of some b.c.c. metals may be modeled by "pencil glide" where the slip direction is confined to <111> directions but the slip plane is not restricted to a particular crystallographic plane (see for example Taylor and Elam (4)). The aim of this paper is to show how a simple modification of the geometry of restricted glide, slip on {110}<111>, has been made to accommodate pencil glide, slip on {hkl}<111>, within the framework of an existing general-purpose computer code for simulation of plastic anisotropy. The principal feature of the model is a strain-rate sensitive single crystal yield surface that permits a Bishop-Hill (1) solution to be used as a trial solution for the pencil glide solution.

A number of studies (3,5-14) have been made to find efficient analytical procedures for solving the pencil glide problem but few have actually gone on to simulate texture evolution under pencil glide conditions (15,16). The geometrical effect of pencil glide can be illustrated by reference to a single crystal yield surface diagram for the three slip systems associated with a single [111] slip direction, Fig. 1. The yield surface for restricted glide is a hexagon whose edges are perpendicular to each {110} slip plane. For pencil glide, however, the yield surface is a circle because the material can always "choose" the slip plane to be that which maximizes the resolved shear stress on the slip system. More general sections of the single crystal yield surface show similarly circular or elliptical shapes (13-15,17). One important consequence of this rounding of the yield surface is that for any given applied stress, the direction of the resulting strain increment will be more nearly parallel to the stress direction than is the case for restricted glide. The significance of this will be apparent when the results of simulation of plane strain compression under Relaxed Constraints boundary conditions are discussed below.

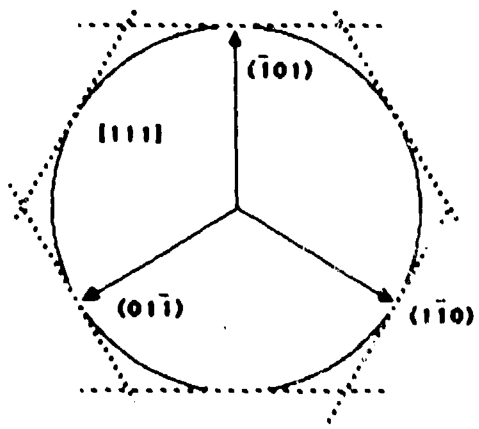

Fig. 1. Single crystal yield surface illustrating difference between restricted glide (hexagon) and pencil glide (circle).

Pencil Glide Simulation

The method of simulating restricted glide in polycrystals with reference to f.c.c. and b.c.c. metals is as follows. For deformation under Full Constraints (FC), using Taylor's assumption of uniform strain in each grain, a Bishop and Hill analysis is used to find the multiple slip stress state, σ^{vertex}, that gives the maximum external work. In order to resolve the ambiguity problem that is a consequence of these assumptions, a non-linear stress strain-rate relation is introduced to round off the single crystal yield surface (18). If the applied strain rate is $\mathbf{D}$, the stress state in a grain σ and the Schmid matrix for the s^{th} slip system $\mathbf{m}^s = \mathbf{b}^s \otimes \mathbf{n}^s$, where $\mathbf{b}^s$ and $\mathbf{n}^s$ are the slip direction and slip plane vectors for the s^{th} slip system respectively, the non-linear solution requires the stress state in each grain to satisfy

$$D_{ij} = \dot{\gamma}_0 \, m_{ij}^s \left(\frac{m_{mn}^s \, \sigma_{mn}}{\tau_0^s} \right)^n \tag{1}$$

A typical value of the exponent, n, is 33; this gives a solution that is essentially rate-insensitive while minimizing the computation effort. The solution procedure starts with a trial value for the stress, calculates a strain rate and uses the difference between this strain rate and the imposed strain rate to adjust the stress state. The solution procedure for Relaxed Constraints (RC) deformation (19,20) is similar; the only difference is that the stress components corresponding to the relaxed strain components are set to zero and the non-linear solution procedure described above is performed in a reduced stress space. Typically three stress components are used instead of the full five components of deviatoric stress space. The solution procedure for pencil glide uses a modified calculation of the resolved shear stress on a slip direction. The resolved shear stress is calculated for each restricted glide slip system as before. What is of interest now, however, is the maximum resolved shear stress, τ^p, that operates on each <111> slip direction when the the slip plane is not restricted. This shear stress is calculated as the vector sum of the three resolved shear stresses calculated above, Fig. 2.

$$\tau^p = \frac{2}{3}\sqrt{|\tau_1 n_1|^2 + |\tau_2 n_2|^2 + |\tau_3 n_3|^2} \tag{2}$$

This results in four different resolved shear stresses associated with each of the four pencil glide slip systems. The resultant shear rate on each system is then obtained from the same strain-rate sensitive formulation as used in restricted glide,

$$\dot{\gamma}^p = \dot{\gamma}_0 \left(\tau^p\right)^n \tag{3}$$

The shear rate is then distributed linearly over the three restricted glide slip systems associated with each pencil glide slip system,

$$\dot{\gamma}^s = \frac{2}{3}\frac{\tau^s}{\tau^p}\dot{\gamma}^p \tag{4}$$

Once a stress state has been found for each grain that satisfies the applied strain increment, Eq. 1, the grain reorientation is calculated in the normal manner.

Results

The model of pencil glide was used to model texture evolution in a simulated b.c.c. polycrystal with 300 grains. Taylor factors were calculated for tension, compression, rolling and torsion with the results given in Table 1. The result for tension and compression are in agreement with those obtained by Parniere and Roesch (3). The Taylor factors for rolling and torsion are given in von Mises equivalent terms, see Tomé et al. (20), and are somewhat lower than for restricted glide.

Table 1.

Deformation Mode	Taylor Factor
tension, compression	2.74
rolling	2.66
torsion	2.60

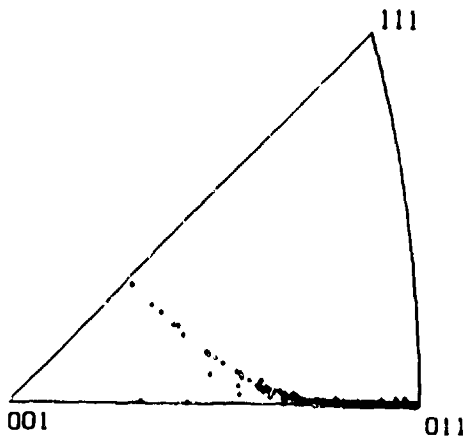

Fig. 3a. Inverse pole figure of orientations of 300 grains simulated with restricted glide to a strain of 2.

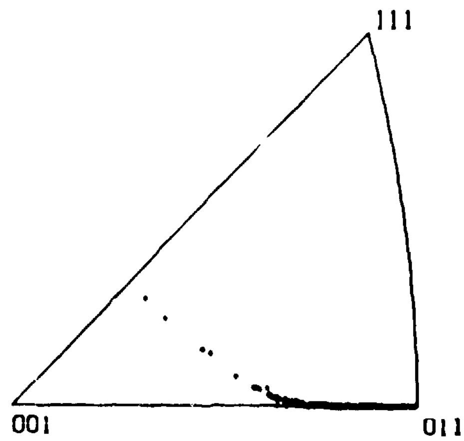

Fig. 3b. Inverse pole figure of simulation of tension with pencil glide to a strain of 2.

The first simulation was performed for tension and gave results that were essentially identical to those for restricted glide, Fig. 3. The same model was used to model rolling (plane strain compression), also with 300 grains. In this case the grain shape evolves to a lath shape and the RC model applies (20). The results are presented in the form of {111} pole figures, Fig. 4, in which the rolling direction and normal direction have been interchanged from their normal positions in order to facilitate comparison with the textures observed for f.c.c. rolling. The simulation performed with restricted glide, Fig. 4a, shows a plane strain texture characteristic of RC simulations, showing "copper" and "S" components. When the simulation is performed with pencil glide, however, there is a subtle change in the texture. Although an increasing fraction of the grains are permitted to deform in Relaxed Constraints as the strain increases, the resulting texture is closer to an FC texture where the principal texture component is shifted to a {11 11 8}<4 4 11> position. This shift can be explained qualitatively as follows. RC deformation permits redundant shears to occur in order to make each grain's stress state more nearly co-linear with the strain direction. The rounded pencil glide single crystal yield surface does not require these redundant shears to satisfy the RC boundary conditions.

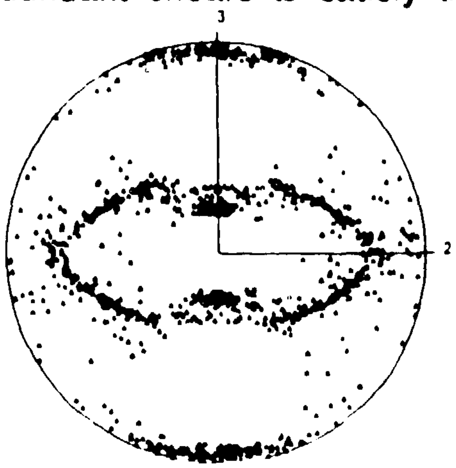

Fig. 4a. {111} pole figure for rolling simulated with 300 grains and restricted glide at a von Mises equivalent strain of 3.

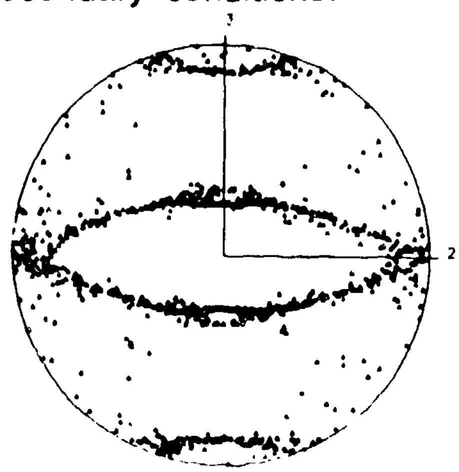

Fig. 4b. {111} pole figure for rolling simulated with 300 grains and pencil glide at a von Mises equivalent strain of 3.

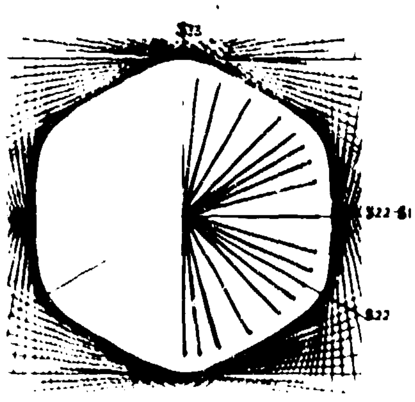

Fig. 5. Yield surfaces in the π-plane for a 300 grain simulated polycrystal. The outer yield surface (tangent planes) corresponds to a Bishop and Hill analysis for restricted glide. The inner yield surface (stress vectors defining a circle) are for pencil glide.

This rounding of the yield surface is also apparent in polycrystal yield surfaces. Figure 5 illustrates the π-plane section of the yield surface for a 300 randomly oriented grains. Two yield surfaces are displayed: the outer tangent plane construction is simply that for restricted glide obtained with the Bishop-Hill analysis and showing the characteristic rounded hexagon. The inner surface is the essentially circular yield surface obtained with pencil glide. The stress vectors whose ends define this inner yield surface are calculated as the mean stress of the polycrystal from the result of the rate-sensitive solution.

Conclusion

The results of this study have shown that pencil glide can be efficiently incorporated into a polycrystal plasticity computer code by adapting the geometry of restricted glide. Texture evolution in tension under pencil glide conditions is very similar to that for restricted glide. For rolling, differences appear at large strains where pencil glide appears to produce a Full Constraints texture even though deformation is permitted to occur in Relaxed Constraints.

References

1. J.F.W. Bishop and R. Hill, Phil. Mag., **42** (1951), 1298-1307.
2. J.M. Rosenberg and H.R. Piehler, Met. Trans., **2** (1971), 257.
3. P. Parnière and L. Roesch, Mem. Sci. Rev. Met., **72** (1975), 221.
4. G.I. Taylor, in Deformation and Flow of Solids, IUTAM Colloq., Madrid, (1955) 3-12.
5. J.W. Hutchinson, J.Mech. Phys. Solids, **12** (1964), 25-33.
6. G.Y. Chin and W.L. Mammel, Trans. AIME, **239** (1967), 1400.
7. H.R. Piehler and W.A. Backofen, Met. Trans., **2** (1971), 249.
8. P. Parnière and C. Sauzay, Mat. Sci. Eng., **22** (1976), 271-280.
9. P. Penning, Met. Trans., **7A** (1976), 1021.
10. P.R. Morris and S.L. Semiatin, Texture Cryst. Solids, **3** (1979), 113-126.
11. S.L. Semiatin, P.R. Morris and H.R. Piehler, Texture Cryst. Solids, **3** (1979), 191-214.
12. F. Royer, C. Tavard and P. Penning, J. Appl. Cryst., **12** (1979), 436-441.
13. J.L. Raphanel and J.-H. Schmitt, Mat. Sci. Eng., **64** (1984), 255-263.
14. P. Gilormini et al., to be published in Acta Met. (1987).
15. I.L. Dillamore and H. Katoh, Met. Sci., **8** (1974), 21.
16. K. Wierzbanowski, Scripta Met., **13** (1979), 1121-1123.
17. U.F. Kocks, Met. Trans., **1** (1970), 1121.
18. G.R. Canova and U.F. Kocks, ICOTOM-7, Holland, (1984) 573.
19. H. Honneff and H. Mecking, ICOTOM-5, Aachen, W. Germany, (1978) 265.
20. C. Tomé, G.R. Canova, U.F. Kocks, N. Christodoulou and J.J. Jonas, Acta Met., **32**, (1984) 1637-1653.